Dynamic Modeling of Deep-Bed Filtration

Previous attempts to model the effect of deposition on removal efficiency in deep-bed filtration have relied heavily on the determination of empirical parameters even for monosized suspensions. A newly developed mathematical model not only significantly reduces this reliance, but takes full account of the polydispersity of suspensions. The results of eight runs on an experimental filter are compraed with the predictions of the mathematical model. Qualitative agreement is good; quantitative agreement is fair.

R. I. Mackie, R. M. W. Horner
Department of Civil Engineering

R. J. Jarvis
Department of Mathematical Sciences
Dundee University
Dundee DD1 4HN, Scotland

Introduction

Over the past fifty years there has been a great deal of research into the mathematical modeling of deep-bed filtration. For a long time most of the work was of an empirical nature (Ives, 1970), but in recent years a more analytical approach has been adopted. Although this has led to some success in predicting the removal efficiency of a clean filter (Rajagopalan and Tien, 1976), there has been little progress toward predicting the dynamic behavior of filters, even for suspensions of monosized particles. Modern models still depend heavily on empirically determined parameters (O'Melia and Ali, 1978). Our purpose has been to develop a model that predicts how the performance of a deep-bed filter varies with time and depth as deposition takes place, but that does not rely on empirical parameters without a physical meaning, and that can deal with suspensions containing particles of various sizes.

In order to validate the mathematical theory, eight experimental runs were conducted on a model filter of 138 mm dia. and 1 m high containing a bed of spherical glass beads. An artificial suspension was made from PVC powder with particles in the size range 0.5 to 15 μm. Superficial velocity was varied between 2.4 and 7.2 m $\cdot$ h^{-1}, and the mean size of the glass beads varied between 0.5 and 1 mm.

A new mathematical model has been developed from a consideration of the physical processes that occur in deep-bed filtration. As a result, the need to rely on empirical parameters that have no physical meaning has been eliminated. The model is based on three main premises:

1. Deposited particles themselves act as collectors. This is not a new idea, but previous workers such as Wang et al. (1977) have calculated the effect of deposited particles by considering each particle individually. We have found that the use of a simple statistical theory leads to a much less complicated computational procedure.

2. It is necessary to consider both the microscopic and macroscopic effect of deposition on a grain, and to model simultaneously both the action of a single deposited particle as a collector and the effect of deposit on the flow field around a grain.

3. Reductions in removal efficiency result primarily from increases in interstitial velocities as deposits grow. This concept was suggested by Stein as long ago as 1940. Since then, it has been common practice to use the change in mean interstitial velocity to characterize the effect. Our model is more sophisticated, and considers the change in fluid velocity near the collector surface. This allows us to incorporate the important precept that the increase in interstitial velocity affects large particles much more than small particles.

The model incorporates one other novel but essential feature: it takes full account of the polydispersity of a suspension, and dispenses with the need to use mean particle diameter as the size characteristic.

Although there are still parameters in the model that currently must be determined experimentally, they have a clearly defined physical meaning. Moreover, we believe that eventually it will be possible to evaluate them mathematically.

The theoretical results are compared with those obtained from a series of experiments. The agreement between theory and experiment is sufficiently good to lend support to the principles on which the mathematical model is based. We therefore conclude that a combination of a dendritic and smooth coating mechanism adequately describes the manner in which solids are deposited within a filter. Our work also confirms that reduction in removal efficiency results primarily from increases in interstitial velocity as deposits grow. Nevertheless, it is inadequate to characterize the effects by changes in mean velocity. Instead it is necessary to consider how the deposits change the tangential fluid velocity near a collector surface. Furthermore, polydispersity of a suspension can be taken into account by evaluating how particles of different sizes are affected by and impinge on the local flow field.

The model is truly predictive since parameter values obtained

Correspondence concerning this paper should be addressed to R. M. W. Horner.

from only one experiment could be used to predict the experimental results for seven different sets of conditions. One of these parameters, v^*, characterizes the fluid velocity at which shear forces inhibit particle deposition. The other, χ_{ij} describes the effect of deposited particles on the local flow field.

We conclude that the accuracy of the model could be improved still further if a constricted-tube model were used in combination with the Happel sphere-in-cell model that we have used, and if a better method of calculating the increase in tangential fluid velocity were developed. The effect of a deposited particle on the local flow field also merits further mathematical investigations.

In summary, the model provides for the first time a real facility for predicting the way in which changes in operating conditions affect filter performance, not only over a reasonably lengthy period of time, but for suspensions made up of particles of different sizes. The model could also be developed to treat suspensions of materially different particles. It also highlights the inadequacy of using a mean diameter to characterize a polydisperse suspension. Particles of different sizes affect filter performance in different ways.

Review of Past Work

The foundations for the mathematical modeling of filtration were laid by Iwasaki (1937) when he proposed that the removal of suspended solids was directly proportional to their concentration. He expressed this mathematically as

$$\frac{\partial C}{\partial \ell} = -\lambda C \tag{1}$$

Ever since Iwasaki it has been common practice to describe the removal efficiency in terms of λ. As particles are removed the filter clogs and the value of λ changes. The degree of clogging is expressed in terms of the specific deposit σ (absolute volume of deposition per unit filter volume). So the mathematical modeling of filtration involves studying the initial rate of removal, λ_o, and examining how λ changes with σ.

Until about fifteen years ago most of the modeling work was of an empirical nature. A good review can be found in Ives (1970). However, these models failed to produce any generally applicable theory. Also, results obtained from filtration experiments are subject to large errors, so any empirical or statistical model that relies on accurate data is at an immediate disadvantage. Over the past fifteen years a more sophisticated treatment has been adopted. The approach has two main elements:

1. The bed is represented by a series of unit bed elements (UBE's), each of length ℓ. Each of these UBE's is in turn considered to be made up of unit collectors, each representing either a grain or a pore in the bed, Figure 1. The removal efficiency of the bed can then be described in terms of the removal efficiency of the unit collectors η. The relationship between λ and η is

$$\lambda = -\frac{1}{\ell}\ln(1-\eta) \tag{2}$$

Single collectors were first used by Yao (1968) and Spielman and coworkers (Spielman and FitzPatrick, 1973). The UBE concept was introduced by Tien and coworkers (Payatakes et al., 1974b; Tien and Payatakes, 1979).

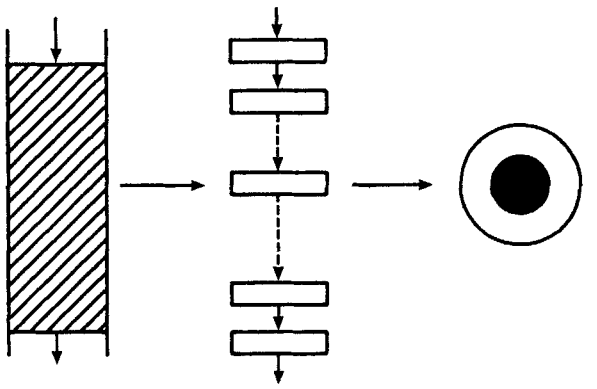

Figure 1. Unit bed element concept.

2. The second element is trajectory analysis. The unit collectors are chosen to have simple geometries (e.g., constricted tubes, Payatakes, 1973, or spheres, Rajagopalan and Tien, 1976) so that the flow field can be calculated. The path of a particle entering the cell can be derived by writing down its equation of motion, taking account of the various forces acting on it, and solving the equation. From this information the fraction of particles entering the cell that will touch the collector can be determined. Multiplying this by the collision efficiency gives the collection efficiency η. The concept of UBE's and trajectory analysis is well described by Tien and Payatakes (1979).

A great deal of valuable work on predicting the initial removal efficiency of a filter has been carried out by Yao (1968), Spielman and FitzPatrick (1973) and Tien and coworkers (Payatakes et al., 1974a, b; Rajagopalan and Tien, 1976). However, the work on predicting how λ changes as the filter becomes clogged is limited. Important work on the early changes in λ has been done by Wang et al. (1977) using dendritic modeling. This is based on the principle that deposited particles themselves act as collectors. However, the work is only applicable to the very early stages of filtration. A model to simulate the complete filter fun was proposed by Tien et al. (1979), but the model still contained a number of empirical parameters. Wnek et al. (1975) presented a model using the Happel (1958) sphere-in-cell unit collector together with a charge balance equation. However, they assumed that the deposit formed a smooth uniform coating around the grains, an assumption that Pendse et al. (1978) have shown to be inadequate.

A feature of the vast majority of the modeling work is that it assumes the suspension to be monodisperse or uses the mean size to characterize the suspension. Horner (1968) and Mackie (1984) show that polydispersity needs to be taken into account.

A mathematical model will now be presented that takes full account of the polydispersity of the suspension, and that does not rely on physically meaningless empirical parameters.

Mathematical Groundwork

Because of its relative simplicity, the unit collector used in this work is the Happel sphere-in-cell model. Not only can it accommodate changes in collector geometry much more easily than the alternative constricted-tube models, but a simple analytical solution for the stream function is available (Happel, 1958). Constricted-tube models, on the other hand, usually

require a numerical solution of the flow field (although Vankatesan and Rajagopalan, 1980, give an analytical solution for the hyperboloidal constricted tube). The Happel model consists of two concentric spheres of radii a and b ($a < b$), where a is chosen to be equal to the radius of a typical grain and b is chosen so that the ratio of the fluid volume between the two spheres to the total volume of the cell is equal to the porosity, f_o, of the clean filter bed. The quantity a is related to b in the following way.

$$a = pb \tag{3}$$

where

$$p = (1 - f_o)^{1/3} \tag{4}$$

The stream function describing the flow, as derived by Happel, is

$$\psi = \frac{1}{2} Va^2 \sin^2\theta \left[k_1 \left(\frac{r}{a}\right)^{-1} + k_2 \left(\frac{r}{a}\right) + k_3 \left(\frac{r}{a}\right)^2 + k_4 \left(\frac{r}{a}\right)^4 \right] \tag{5}$$

where

$$k_1 = \frac{1}{w}, \quad k_2 = -(3 + 2p^5)/w,$$

$$k_3 = (2 + 3p^5)/w, \quad k_4 = -p^5/w$$

and

$$w = 2 - 3p + 3p^5 - 2p^6$$

V is called the approach velocity for the Happel model. It has been common practice to take V to be equal to U, the superficial velocity of the flow through the filter. However, Mackie (1984) has shown that Eq. 6 expresses the correct relationship between V and U (see the Appendix):

$$V = \left(\frac{4}{3}\right)^{2/3} \left(\frac{1}{\pi}\right)^{1/3} U \tag{6}$$

The majority of the work in this paper will be presented in dimensionless variables. Distances are made dimensionless by dividing by the grain radius a, so $\bar{r} = r/a$. The collector and outer sphere radii are now 1 and p^{-1}. The dimensionless stream function is

$$\bar{\psi} = \frac{\psi}{Va^2} \frac{1}{2} = \sin^2\theta (k_1 \bar{r}^{-1} + k_2 \bar{r} + k_3 \bar{r}^2 + k_4 \bar{r}^4) \tag{7}$$

Trajectory analysis in general requires a numerical solution of the equation of motion. For a clean filter this is not a serious problem. However, when deposition occurs the shape of the collector changes, and causes a change in the flow field. It would be much easier to take account of these changes if an analytical solution of the equation of motion were available. Such a solution is available if the hydrodynamic drag force on particles is assumed to be given by Stokes' law (i.e., drag corrections are ignored) and if the London and double-layer forces are ignored. Although Rajagopalan and Kim (1981) have shown that for colloidal particles, surface forces are significant, Rajagopalan and Tien (1977) concluded that for larger particles the surface forces are important only in determining whether or not conditions for deposition are favorable, not in determining its magnitude. Under this simplifying assumption the path of a particle is given by

$$\bar{\psi} + \tfrac{1}{2} N_G \bar{r}^2 \sin^2\theta = A \tag{8}$$

where $N_G = (\rho_p - \rho) g a_p^2 / 18\mu V$, the gravity paremeter, and A is a constant. Given any position through which the particle passes, say (r_o, θ_o), A can be calculated and Eq. 8 then defines the complete trajectory. $\bar{\psi} + \tfrac{1}{2} N_G \bar{r}^2 \sin^2\theta$ is a stream function defining the motion of the suspended particles. The quantity A will be referred to as the trajectory parameter. Equation 8 is a very useful tool, but it should always be borne in mind that the hydrodynamic retardation effect has been ignored.

It is known that under the above conditions the limiting trajectory passes through $(1 + N_R, \pi/2)$ (Yao, 1968), where $N_R = a/a_p$. So the path of the limiting trajectory can be found using Eq. 8 and the collection efficiency can be calculated. The result is

$$\eta_o = 2A_{\text{lim}} p^2 / a^2 (1 + N_G) \tag{9}$$

where A_{lim} is the limiting trajectory parameter and is given by

$$A_{\text{lim}} = \bar{\psi}\left(1 + N_R, \frac{\pi}{2}\right) + \frac{1}{2} N_G (1 + N_R)^2 \tag{10}$$

It has been standard practice (Rajagopalan and Tien, 1976) to relate λ to η by

$$\lambda = \frac{-3}{4a} (1 - f_o) \ln (1 - \eta) \tag{11}$$

but the correct relationship is in fact expressed in Eq. 12 (see the Appendix):

$$\lambda = -\left(\frac{3}{4}\pi\right)^{1/3} \frac{p}{a} \ln (1 - \eta) \tag{12}$$

All the above work is described in detail in Mackie (1984). It is also shown there that this simplified form of trajectory analysis predicts that the change in shape of the collector in the very early stages of deposition will be

$$\bar{r} = \begin{cases} 1 + \epsilon \cos\theta + 0(\epsilon^2) & \theta \in [0, \pi/2] \\ 1 & \theta \in [\pi/2, \pi] \end{cases} \tag{13}$$

where ϵ is a measure of the amount of deposition, discussed later. Equation 13 defines a dome shape and deposition has been observed to occur in this form by Ison and Ives (1969).

For the early stages of deposition the Happel model should prove effective as it is well suited to modeling the dome shape of the deposit. Later on, however, constriction and possibly blocking of the pores become important (Maroudas and Eisenklam, 1965; Payatakes et al., 1981) and the constricted-tube models are appropriate. Therefore it should not be surprising if the Happel model does not work well in the later stages of filtration.

In the present work it will be assumed that the shape of the

deposit is described by

$$\bar{r} = \begin{cases} 1 + \epsilon \cos\theta - \epsilon^2 \cos^2\theta & \theta \in [0, \pi/2] \\ 1 & \theta \in [\pi/2, \pi] \end{cases} \quad (14)$$

throughout the filter run. For small ϵ Eq. 14 is equivalent to Eq. 13 and so is a good description of the early stages. The term $-\epsilon^2 \cos^2\theta$ has the effect of giving a more "rounded" shape to the deposit. Calculation of the shape of the deposit in the later stages is difficult or impossible, and so Eq. 14 will be used for the sake of simplicity.

Model Description

A qualitative description of the model will be followed by a more detailed description of the calculations involved. The model consists of three main elements:

1. Simplified dendritic modeling
2. A combination of dendritic and smooth coating deposition
3. The effect of increased interstitial velocity on removal efficiency

Simplified dendritic modeling

It is well established that deposited particles themselves act as collectors (Payatakes et al., 1981), and detailed models have been developed to calculate the effect of deposited particles on collection efficiency (Wang et al., 1977). However, these models are very complex because they consider each particle individually. In the present model simple probability theory is used to calculate the "average" effect of deposited particles on collection efficiency. Dendritic modeling was originally developed for air filtration, where chains of particles have been observed to form (Payatakes and Tien, 1976). In water filtration the viscous forces are much greater, so it will be assumed that "dendrites" of only one particle in length are formed. This greatly simplifies the calculations and still gives good results.

Combined dendritic and smooth coating deposition

Dendritic modeling is the best description for the very early stages of deposition, but what is the best approach when there is a significant amount of deposit on the grain?

Consider a grain with deposit on it. If this grain could be looked at from a distance it would look like Figure 2a. However, if a closer look at one part of the grain were taken it would look like Figure 2b. Therefore the answer to the question is that the smooth dome shape gives a good general description of the deposit, but the dendritic approach is needed to describe the microscopic nature of the deposit. So a model of the effect of deposition on removal must combine the dome shape and the dendritic approach. Such a combination is incorporated in the model presented herein.

Effect of increased interstitial velocity

Many researchers have taken the view that the increase in interstitial velocity in a filter is responsible for the decrease in removal efficiency (Stein, 1940; Ives, 1960; Tien et al., 1979). However, models have used the mean interstitial velocity to characterize the effect. We believe this to be too simplistic and adopt a more sophisticated approach.

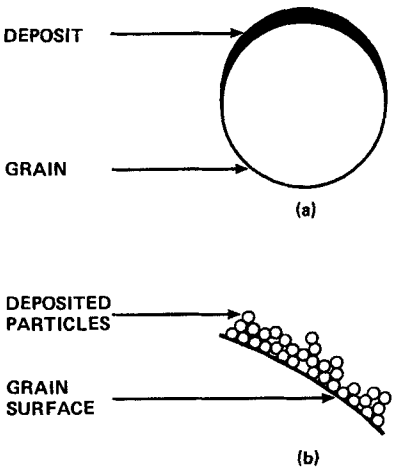

Figure 2. Deposit on a grain.
a. Macroscopic view
b. Microscopic view

Consider a particle of radius a_p just about to touch the collector surface at a point P. If v_θ is the tangential fluid velocity at a distance a_p above the surface at P, then the tangential drag force F acting on the particle is (Goldman et al., 1967)

$$F_\theta = 1.7005 \times 6\pi\mu a_p v_\theta \quad (15)$$

It is suggested that when F_θ reaches a critical value F^*, then particles of size a_p can no longer deposit at the point P. Now as deposition builds up the only variable in Eq. 15 that changes is v_θ. We therefore make the following hypothesis:

Hypothesis. For particles of size a_p there exists a critical velocity v^* such that particles of size a_p cannot adhere to any point on a grain at which the tangential velocity at a distance a_p above the surface is greater than or equal to v^*.

Now v_θ has different values at different points on the grain, so at any time in a filter run for particles of a given size there are three possibilities:

1. $v_\theta < v^*$ everywhere; i.e., deposition is unhindered
2. $v_\theta \geq v^*$ on part of the grain; i.e., deposition can occur on only part of the grain
3. $v_\theta \geq v^*$ on all of the grain; i.e., deposition has stopped

Note that the above refers only to the part of the grain $0 \leq \theta \leq \pi/2$, as under our assumptions deposition can never occur beyond $\theta = \pi/2$.

It is not possible to calculate v^* exactly due to the complexity of the adhesion forces between a particle and a grain. The critical velocity v^* has therefore to be found empirically.

Since we intend to develop a model to deal with polydisperse suspensions we need to ask, "How does v^* vary with particle size"? The dominant force in adhesion is the London force. Since the particles are much smaller than the grains, for the purposes of calculating the adhesion force the situation can be likened to that of a sphere just touching a plane. The London force is then

$$F_{\text{Lon}} = Ha_p/6z_o^2 \quad (16)$$

where z_o is the distance of minimum separation. For smooth surfaces Visser (1976) found that the shear force F^* needed to dis-

lodge a particle was equal to the London force. So v^* is given by

$$1.7005 \times 6\pi\mu a_p v^* = Ha_p/6z_o^2$$

$$v^* = H/(1.7005 \times 36 \times \pi\mu z_o^2) \quad (17)$$

Thus, if z_o is independent of a_p, v^* is also independent of a_p. For particles made of the same material this is likely to be the case. Now the situation in a filter is more complex than that considered above, but as a first approximation it is reasonable to assume that v^* is independent of size. However, this does not mean that the deposition of all particle sizes at a particular point stops simultaneously. The fluid velocity is zero at the collector surface and increases as one moves away from the surface toward the middle of the pore. Therefore since larger particles protrude farther into the flow they are acted on by faster moving fluid. This implies that the deposiiton of large particles will decrease before that of small ones.

Simplified dendritic modeling—calculations

Consider the suspension to be made up of particles of (dimensionless) size

$$d_1, d_2, \ldots, d_n \quad (18)$$

where $d_1 < d_2 < \cdots < d_n$ and assume that the relative concentrations of the particle sizes in vol/vol terms are

$$C_1, C_2, \ldots, C_n \quad (19)$$

Consider a single particle of size d_i deposited on an otherwise clean collector at $(1, \theta_o, \phi_o)$ (using spherical polar coordinates). What is the effect of this particle on trajectories in the half-plane $\phi = \phi_o$? Consider the effect on particles of size d_j. Then if d_i is the diameter of the deposited particle, the limiting trajectory for capture by the deposited particle passes through $(1 + d_i + N_{Rj}, \theta_o, \phi_o)$, where N_{Rj} is the interception parameter for particles of size d_j. Let $A_{ij}(\theta_o)$ be the associate trajectory parameter. First assume that the flow field is undisturbed by the deposited particles. Then

$$A_{ij}(\theta_o) = \psi_o(1 + d_i + N_{Rj}, \theta_o) + \tfrac{1}{2}N_{Gj}(1 + d_i + N_{Rj})^2 \sin^2\theta_o \quad (20)$$

where ψ_o is the stream function defined by Eq. 7, and N_{Gj} is the gravity parameter for particles of size d_j. The collection efficiency is

$$\eta_{ij}(\theta_o) = 2A_{ij}(\theta_o)p^2/(1 + N_{Gj}) \quad (21)$$

Let η_{oj} be the initial collection efficiency for particles of size d_j. Let $\eta_{\phi ij}$ be the collection efficiency for trajectories in the half-plane ϕ_o. Then if

$$\eta_{ij}(\theta_o) \geq \eta_{oj}, \quad \eta_{\phi ij} = \eta_{ij}(\theta_o), \quad \text{and if } \eta_{oj} > \eta_{ij}(\theta_o), \quad \eta_{\phi ij} = \eta_o,$$

i.e.,

$$\eta_{\phi ij} = \max\,[\eta_{oj}, \eta_{ij}(\theta_o)] \quad (22)$$

or

$$= 2A_{\phi ij}p^2/(1 + N_{Gj}) \quad (23)$$

where

$$A_{\phi ij} = \max\,[A_{oj}, A_{ij}(\theta_o)] \quad (24)$$

with

$$A_{oj} = \eta_{oj}(1 + N_{Gj})/2p^2 \quad (25)$$

The value of $\eta_{\phi ij}$ will vary depending on the position of the deposited particle. What is the expected value of $\eta_{\phi ij}$? From Eq. 13 it can be deduced that the probability density function (PFD) of θ_o is $2 \cos\theta_o \sin\theta_o$, therefore

$$\bar{\eta}_{ij} = \int_o^{\pi/2} 2\eta_{\phi ij} \cos\theta_o \sin\theta_o d\theta_o \quad (26)$$

where $\bar{\eta}_{ij}$ is the mean value of $\eta_{\phi ij}$.

In reality, the deposited particle will affect the local flow field. The parameters $A_{ij}(\theta_o)$ will therefore be multiplied by some value χ_{ij} to take account of this. Thus $A_{ij}(\theta_o)$ should be replaced by

$$A'_{ij}(\theta_o) = \chi_{ij}A_{ij}(\theta_o) \quad (27)$$

in all the above calculations. The values of ψ_{ij} are discussed later.

This describes the effect of one particle on one trajectory half-plane. But each deposited particle will affect only a fraction of all the trajectory half-planes, and its effect on each of these will be different. Consider a particular trajectory half-plane ϕ_o. What is the probability of one particular deposited particle affecting this half-plane? It will be assumed that for this particle to affect trajectories in this half-plane its center must lie within a distance $d_i/2$ of ϕ_o, i.e., some part of the deposited particle lies in the half-plane ϕ_o. The protrusion of this particle above the collector is d_i only in the particular half-plane in which its center lies. What is the average protrusion? Or, what is the "average height" of a particle? Since the particle is small compared to the collector, it can be assumed that the collector is a half-plane. Let y_i be the protrusion at any point, Figure 3, then $y_i = d_i/2(1 + \sin\theta)$ and the average value of y_i

$$d'_i = d_i\left(\frac{1}{2} + \frac{1}{\pi}\right) \quad (28)$$

d'_i will now be used instead of d in all calculations such as Eq. 20.

Now suppose that there are n_i particles of size $d_i (i = 1, \ldots, n)$ on the collector. What is the total effect of these particles on the collection efficiency? Suppose a particle of size d_i is deposited at $\theta = \theta_o$. Then the circle $\theta = \theta_o$, $r = 1$, has radius $\sin\theta_o$ and circumference $2\pi \sin\theta_o$. For the deposited particle to affect a particular trajectory half-plane, ϕ_o, it must be within a distance $d_i/2$ of ϕ_o. If $d_i < 2\pi \sin\theta$ then a length d_i of the circle is within $d_i/2$ of ϕ_o. If $d_i > 2\pi \sin\theta$ all of the circle is within $d_i/2$ of ϕ_o. Therefore the

y = height above grain surface

x = grain diameter

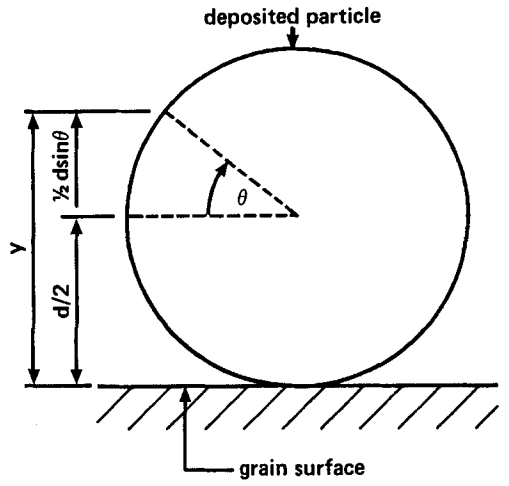

Figure 3. Average height of a sphere.

probability of a particle affecting the half-plane is

$$P_i = \begin{cases} d_i/2\pi \sin\theta & d_i \le 2\pi \sin\theta \\ 1 & d_i > 2\pi \sin\theta \end{cases} \tag{29}$$

The mean value of P_i for θ $[0, \pi/2]$ is

$$\bar{P}_i = \frac{d_i}{\pi}(1 - d_i/4\pi) \tag{30}$$

Let P_{0i} be the probability of no particles of size d_i affecting the half-plane ϕ_o, and let P_{1i} be the probability of at least one particle affecting the half-plane. P_{0i} and P_{1i} are given by

$$P_{0i} = (1 - \bar{P}_i)^{n_i}, \quad P_{1i} = 1 - P_{0i} \tag{31}$$

The overall collection efficiency for particles of size d_j can now be calculated as follows. First arrange the $\bar{\eta}_{ij}(i = 1, 2, \ldots, m)$ in ascending order of magnitude

$$\bar{\eta}_{i_1 j} < \bar{\eta}_{i_2 j} < \cdots < \bar{\eta}_{i_m j} \tag{32}$$

i.e., particles of size d_{i_m} have the greatest average effect on collection efficiency. Therefore as an approximation it will be assumed that if particles of size d_{i_m} have been deposited on the grain, the new collection efficiency is given by $\bar{\eta}_{i_m j}$, the mean effect of particles of size d_{i_m}. If there are no new deposited particles of size d_{i_m}, but there are particles of size $d_{i_{m-1}}$, the new collection efficiency will be taken to be $\bar{\eta}_{i_{m-1} j}$. This process is repeated until the possibility of no particles at all affecting the half-plane is considered. The new collection efficiency will be given by the expected value of η_j, which can be calculated as follows.

Let $P_{i_k j}$ be the probability of a trajectory half-plane being affected by particles of size d_{i_ℓ} but not by particles of size d_{i_k}, where $k > \ell$. Then

$$P_{i_m j} = P_{1,i_m}$$

$$P_{i_k j} = P_{0,i_m} \cdot P_{0,i_{m-1}} \cdots P_{0,i_{k+1}} \cdot P_{1,i_k} \quad \ell = 1, 2, \ldots, m-1 \tag{33}$$

and the probability of no particles at all affecting the trajectory is

$$P_0 = P_{0m}, P_{0m-1}, \ldots, P_{01} \tag{34}$$

Then the collection efficiency for particles of size d_j is

$$\eta_j = P_o \eta_{oj} + \sum_{\ell=1}^{m} P_{i_k j} \bar{\eta}_{i_k j} \tag{35}$$

Combined dendritic and smooth coating deposition

The calculations above describe a simple method of treating the deposit dendritically. We now describe how to calculate the collection efficiency when there is a significant amount of deposit on the grains. It was explained earlier that the deposition has to be viewed both as a smooth dome shape, and dendritically. Suppose that the specific deposit at some layer in the filter is σ, and that the filter coefficients for the various particle sizes are $\lambda_{\sigma i}$. Let $\eta_{\sigma i}$ be the corresponding collection efficiencies for the Happel model. The effect of further deposition on removal efficiency is calculated as follows.

Consider the Happel model when the solid collector has the deformed shape

$$r = \begin{cases} 1 + \epsilon_\sigma \cos\theta - \epsilon_\sigma^2 \cos^2\theta & \theta \in [0, \pi/2] \\ 1 & \theta \in [\pi/2, \pi] \end{cases} \tag{36}$$

The quantity ϵ_σ is chosen so that the volume of the deformed collector is the same as that of the grain plus deposit. Let V_ϵ be the volume of the solid described by Eq. 36. Then

$$V_\epsilon = 4\pi/3 + \pi\epsilon_\sigma + 0(\epsilon_\sigma^3) \tag{37}$$

The total volume of the Happel model is $4\pi/3(1 - f_o)$, so the bulk volume of the deposit is $4\pi\sigma/3(1 - f_o)(1 - f_d)$, where f_d is the porosity of the deposit. From Eq. 37 the volume is also $\pi\epsilon_\sigma$, therefore

$$\epsilon_\sigma = 4\sigma/3(1 - f_o)(1 - f_d) \tag{38}$$

The flow field will also have changed because of the deposition. It is possible to obtain a perturbation solution for the new stream function (Mackie, 1984), but the solution is valid only for small ϵ, and to go to higher order approximations is complicated. Instead, the following method is used to calculate the value of the new stream function, ψ_σ, at the point $(1 + \epsilon_\sigma \cos\theta_o - \epsilon_\sigma^2 \cos^2\theta_o + x, \theta_o, \phi_o)$ i.e., at a distance x above the collector surface.

The interval $[1 + \epsilon_\sigma \cos\theta - \epsilon_\sigma^2 \cos^2\theta_o p^{-1}]$ can be mapped to $[1, p^{-1}]$ by the function

$$g(r) = 1 + \frac{(p^{-1} - 1)(r - 1 - \epsilon_\sigma \cos\theta + \epsilon_\sigma^2 \cos^2\theta)}{(p^{-1} - 1 - \epsilon_\sigma \cos\theta + \epsilon_\sigma^2 \cos^2\theta)} \tag{39}$$

The value of ψ_σ at $(1 + \epsilon_\sigma \cos\theta_o - \epsilon_\sigma^2 \cos^2\theta + x, \theta_o, \phi_2)$ is now

taken to be:

$$\psi_\sigma(1 + \epsilon_\sigma \cos\theta_o - \epsilon_\sigma^2 \cos^2\theta_o + x, \theta_o) = \psi_\sigma[g(1 + \epsilon_\sigma \cos\theta_o - \epsilon_\sigma^2 \cos^2\theta_o + x), \theta_o] = \psi_\sigma\left[1 + \frac{x(p^{-1} - 1)}{(p^{-1} - 1 - \epsilon_\sigma \cos\theta_o + \epsilon_\sigma^2 \cos^2\theta_o)}, \theta_o\right] \quad (40)$$

The accuracy of Eq. 40 is discussed later.

As before, consider the effect of a single particle of size d_i deposited on a collector whose shape is defined by Eq. 36 at $(1 + \epsilon_\sigma \cos\theta_o - \epsilon_\sigma^2 \cos^2\theta_o, \theta_o, \phi_o)$. The limiting trajectory for capture by this particle of particles of size d_j passes through $(1 + \epsilon_\sigma \cdot \cos\theta_o - \epsilon_\sigma^2 \cos^2\theta_o + N_{Rj} + d_i, \theta_o, \phi_o)$. Let $A_{ij}(\theta_o)$ be the associated trajectory parameter, then

$$A_{ij}(\theta_o) = \psi_o\left\{1 + \frac{x_{ij}(p^{-1} - 1)}{[p^{-1} - (1 + \epsilon_\sigma \cos\theta_o - \epsilon_\sigma^2 \cos^2\theta_o)]}, \theta_o\right\} + \frac{1}{2} N_{Gj}(1 + \epsilon_\sigma \cos\theta_o - \epsilon_\sigma^2 \cos^2\theta + x_{ij})^2 \sin^2\theta_o \quad (41)$$

where

$$x_{ij} = d_i + N_{Rj} \quad (42)$$

To account for the effect of the deposited particles on the local flow field, $A_{ij}(\theta)$ is multiplied by χ_{ij} to give

$$A'_{ij}(\theta) = \chi_{ij} A_{ij}(\theta) \quad (43)$$

Let

$$A_{\phi_o ij} = \max\,[A_j(\sigma), A'_{ij}(\theta)] \quad (44)$$

where

$$A_j(\sigma) = \eta_j(\sigma)(1 + N_{Gj})/2p^2 \quad (45)$$

Then the collection efficiency for the trajectories in the half-plane ϕ_o is

$$\eta_{\sigma_o ij} = 2A_{\phi_o ij} p^2/(1 + N_{Gj}) \quad (46)$$

As before $\eta_{\phi_o ij}$ will vary with θ_o. The PDF of θ_o will in fact have changed, but for the sake of simplicity the function $2\cos\theta_o \sin\theta_o$ will still be used. The expected value of $\eta_{\phi ij}$ is then

$$\bar{\eta}_{ij} = \int_o^{\pi/2} 2\eta_{\phi_o ij} \cos\theta \sin\theta \, d\theta \quad (47)$$

Again only one half-plane has so far been considered. Now suppose that n_i particles of size $d_i (i = 1, \ldots, m)$ have been deposited on the collector since the deposit was σ. As before, replacing d_i by d'_i and defining the probabilities by Eqs. 29–34 (the effect of deposition on the value of P_i is ignored), the overall collection efficiency for particles of size d_j is

$$\eta_j = P_o \eta_j(\sigma) + \sum_{i=1}^{m} P_{i_k j} \eta_{i_k j} \quad (48)$$

Eventually enough particles will have deposited on the deformed collector to render it necessary to change the value of ϵ_σ in Eq. 36. Suppose it is necessary to do this when the specific deposit is $\sigma + \delta\sigma$. Let $\eta_{\sigma+\delta\sigma ij}$ be the value of η_j obtained using Eq. 48. To consider the effect of further deposition the above process can be repeated with $\sigma + \delta\sigma$, $\eta_{\sigma+\delta\sigma ij}$ and $\epsilon_{\sigma+\delta\sigma}$ in place of σ, $\eta_{\sigma j}$, and ϵ_σ, respectively. By this means, starting from $\sigma = 0$ the effect of deposition on removal efficiency can be calculated by changing the shape of the collector when $\sigma = \delta\sigma_o, 2\delta\sigma_o, \ldots$. The choice of $\delta\sigma_o$ is discussed later.

Effect of shear forces

It was hypothesized in the qualitative description of the model that when the tangential fluid velocity at a distance a_p above a point on a collector reaches a critical value v^*, then particles of radius a_p can no longer deposit at that point. Given that v^* is known, the effect of deposition on interstitial velocity and hence on removal efficiency will now be calculated. Consider a particle of diameter d_i just about to touch the clean collector at a point $(1, \theta_o, \phi_o)$. The tangential fluid velocity of the fluid at $(1 + d_i/2, \theta_o)$ is

$$v_{\theta_o} = \frac{\sin\theta_o}{2}(-k_1 r^{-3} + k_2 r^{-1} + 2k_3 + 4k_4 r^2)|_{r=1+d_i/2} = h(1 + d_i/2)\sin\theta_o \quad (49)$$

where

$$h(r) = 0.5(-k_1 r^{-3} + k_2 r^{-1} + 2k_3 + 4k_4 r^2) \quad (50)$$

Increases in the volume of deposit lead to increases in interstitial velocity. As with the effect of deposition on the stream function, a very simple procedure will be used to calculate this increase. Consider a section of the cell defined by $\theta = \theta_o$. Let $S^\epsilon_{\theta_o}$ be the area of the section

$$1 + \epsilon \cos\theta_o - \epsilon^2 \cos^2\theta_o \le r \le p^{-1} \quad (51)$$

This is the area between the collector surface and the outer boundary of the cell, i.e., the area available for flow. Then

$$S^\epsilon_\theta = \pi[p^{-2} - (1 - \epsilon\cos\theta_o - \epsilon^2\cos^2\theta)^2]\sin\theta_o \quad (52)$$

Let S^o_θ be the value of S^ϵ_θ for the clean collector, and let v^o_θ be the value of v_θ when $\epsilon = 0$, given by Eq. 49. Let S^ϵ_θ and v^ϵ_θ be the corresponding value for ϵ. It is now assumed that

$$\frac{v^\epsilon_\theta}{v^o_\theta} = \frac{S^o_\theta}{S^\epsilon_\theta} \quad (53)$$

i.e., it is assumed that the tangential fluid velocity is inversely proportional to the area available for flow, S^ϵ_θ. Therefore the tangential velocity v^ϵ_θ at a distance $d_i/2$ above the collector surface is given by

$$v^\epsilon_\theta = \frac{(p^{-2} - 1)}{[p^{-2} - (1 + \epsilon\cos\theta - \epsilon^2\cos^2\theta)^2]} \cdot h(1 + d_i/2)\sin\theta \quad (54)$$

The accuracy of v^ϵ_θ is discussed later.

Consider the part of the grain defined by $\theta = \theta_o$. Deposition of particles of size d_i will stop at $\theta = \theta_o$ when $v_\theta' \geq v^*$. If $h(1 + d_i/2) \sin\theta_o \geq v^*$, then particles of size d_i can never deposit at θ_o. Otherwise the critical value of ϵ at which deposition of particles of size d_i stops at θ_o is given by [ignoring terms of $0(\epsilon^3)$]

$$\epsilon_i^* = \frac{v^* - \sqrt{v^{*2} - (p^{-2} - 1)[v^* - h(1 + d_i/2)\sin\theta_o]v^*}}{v^* \cos\theta_o} \tag{55}$$

Thus, given ϵ the part of the collector where deposition cannot take place can be calculated.

Because $h(1 + d_i/2)$ varies with d_i, ϵ_i^* also varies with d_i. So although v^* was assumed to be the same for all sizes, ϵ_i^* is size-dependent, ϵ_i increasing as d_i decreases.

The part of the collector on which particles cannot deposit (excluding the region $(\pi/2, \pi J)$ will be called the region of no deposition. Since there are m different sizes of particles there will be m different regions of no deposition (although some of them will be null sets if deposition is unhindered for certain sizes). When $\sigma = \sigma_{k-1}$ let these regions be denoted by

$$\theta_{1ik-1} \leq \theta \leq \theta_{2ik-1} \quad i = 1, 2, \ldots, m \tag{56}$$

(Calculations indicate that the regions are continuous; Mackie, 1984.)

In Eq. 36 ϵ was independent of θ. However, now that there are regions of no deposition ϵ is also dependent upon θ. Suppose that when $\sigma = \sigma_{k-1}$ the collector had the shape

$$r = \begin{cases} 1 + \epsilon_{k-1}(\theta)\cos\theta - \epsilon_{k-1}(\theta)^2 \cos^2\theta & \theta \in [0, \pi/2] \\ 1 & \theta \in [\pi/2, \pi] \end{cases} \tag{57}$$

What is the shape when $\sigma = \sigma_k = \sigma_{k-1} + \delta\sigma$? $\delta\sigma$ can be written as

$$\delta\sigma = \delta\sigma_1 + \delta\sigma_2 + \cdots + \delta\sigma_m \tag{58}$$

where $\delta\sigma_i$ is the part of the increase in σ caused by the deposition of particles of size d_i. If η_{ik-1} $(i = 1, \ldots, m)$ are the collection efficiencies when $\sigma = \sigma_{k-1}$, then $\delta\sigma_i$ is given by

$$\delta\sigma_i = \frac{C_i \eta_{ik-1} \delta\sigma}{\sum_{j=1}^{m} C_j \eta_{jk-1}} \tag{59}$$

The number of particles of size d_i is

$$n_i = \frac{8\delta\sigma_i}{(1 - f_o)\, d_i^3} \tag{60}$$

Let

$$\epsilon_k(\theta) = \epsilon_{k-1}(\theta) + \delta\epsilon(\theta) \tag{61}$$

where

$$\delta\epsilon = \delta\epsilon_1 + \cdots + \delta\epsilon_m \tag{62}$$

$\delta\epsilon_i$ being the increase in ϵ associated with $\delta\sigma_i$. None of the deposition $\delta\sigma_i$ has occurred on $(\theta_{1ik-1}, \theta_{2ik-1})$, so $\delta\epsilon_i = 0$ in this region. If $\delta\sigma$ is small it can be assumed that $\delta\epsilon_i$ is constant for $\theta \notin (\theta_{1ik-1}, \theta_{2ik-1})$. Let δv_i be the change in volume associated with $\delta\sigma_i$, then

$$\delta v_i = \pi \delta\epsilon_i \alpha_{ik-1} + 0(\delta\epsilon^3) \tag{63}$$

where

$$\alpha_{ik} = 1 - (\sin^2\theta_{2ik} - \sin^2\theta_{1ik}) \tag{64}$$

α_{ik} is a measure of the importance of the region of no deposition for particles of size d_i. When deposition is unhindered $\alpha_{ik} = 1$. When deposition stops altogether $\alpha_{ik} = 0$. The value of δv_i is also given by

$$\delta v_i = \frac{4\pi\delta\sigma_i}{3(1 - f_o)\,(1 - f_d)} \tag{65}$$

(including the porosity of the deposit). Therefore

$$\delta\epsilon_i = \frac{4\delta\sigma_i}{3(1 - f_o)\,(1 - f_d)\alpha_{ik-1}} \quad \theta \notin (\theta_{1ik-1}, \theta_{2ik-1}) \tag{66}$$

Thus the shape of the collector can be calculated and, using Eq. 55, so can the region of no deposition $(\theta_{1ik}, \theta_{2ik})$ when $\sigma = \sigma_k$.

The effect of the regions of no deposition on collection will now be calculated. Suppose that when $\sigma = \sigma_{k-1}$ the collection efficiencies for the different particle sizes were η_{jk-1}. We need to decide what happens to the particles that would normally be deposited on the region of no deposition. There are three possibilities.

1. None are collected
2. Some are collected elsewhere on the collector
3. All are collected elsewhere on the collector

Initially the first possibility will be assumed, but later this will be modified.

As σ increases from σ_{k-1} to σ_k the region of no deposition will increase in size from $(\theta_{1jk-1}, \theta_{2jk-1})$ to $(\theta_{1jk}, \theta_{2jk})$. η_{jk-1} will be modified to η_{jk-1}^*, where

$$\eta_{jk-1}^* = \eta_{jk-1}\, \alpha_{jk}/\alpha_{jk-1} \tag{67}$$

A_{jk-1} is similarly modified to A_{jk-1}^*.

The effect of a single particle of size d_i deposited at $(1 - \epsilon\cos\theta_o + \epsilon^2\cos^2\theta_o, \theta_o, \phi_o)$ also needs to be modified. Consider its effect on the collection efficiency for particles of size d_j. Let $(\theta_{1ik}, \theta_{2ik})$ and $(\theta_{1jk}, \theta_{2jk})$ be the regions of no deposition for particles of size d_i and d_j, respectively. If $\theta_o \in (\theta_{1jk}, \theta_{2jk})$, particles of size d_j cannot be captured by the deposited particles. Therefore the collection efficiency remains the same, i.e.,

$$A_{ij}^*(\theta_o) = A_{jk-1}^* \tag{68}$$

If $\theta_o < \theta_{1jk}$, the region $(\theta_{1jk}, \theta_{2jk})$ has no effect on collection efficiency and

$$A_{ij}^*(\theta_o) = \chi_{ij} A_{ij}'(\theta_o) \tag{69}$$

where $A_{ij}(\theta_o)$ is defined by Eq. 41. If $\theta_o > \theta_{2jk}$, Eq. 69 needs to be modified to take account of the fact that particles of size d_j can-

not deposit on $(\theta_{1jk}, \theta_{2jk})$ so $A'_{ij}(\theta_o)$ will be multiplied by α_{jk}. Then

$$A^*_{ij}(\theta_o) = \chi_{ij} A'_{ij}(\theta_o)\, \alpha_{jk} \tag{70}$$

As before

$$A_{\phi ij} = \max\, [A^*_{jk-1}, A^*_{ij}(\theta_o)] \tag{71}$$

and

$$\eta_{\phi ij} = 2A_{\phi ij} p^2/(1 + N_{Gj}) \tag{72}$$

Since particles of size d_i cannot deposit on $(\theta_{1ik}, \theta_{2ik})$ the PDF of θ_o is changed to $2 \cos \theta_o \sin \theta_o/\alpha_i$, and $\bar{\eta}_{ij}$ is now given by

$$\bar{\eta}_{ij} = \frac{1}{\alpha_{ik}} \int_0^{\pi/2} 2\eta_{\phi ij} \cos \theta_o \sin \theta_o I_i(\theta_o)\, d\theta_o \tag{73}$$

where

$$I_i(\theta_o) = \begin{cases} 1 & \theta_o \notin (\theta_{1ik}, \theta_{2ik}) \\ 0 & \theta \in (\theta_{1ik}, \theta_{2ik}) \end{cases} \tag{74}$$

The definition of $\bar{P}_i$ is changed to

$$\bar{P}_i = \frac{1}{\alpha_{ik}} \int_o^{\pi/2} 2P_i \cos \theta_o \sin \theta_o I_i(\theta_o)\, d\theta_o \tag{75}$$

where $\bar{P}_i$ is defined by Eq. 29.

So far it has been assumed that none of the particles that would otherwise have deposited on the region of no deposition are collected. In reality it is probable that some of the particles will be collected elsewhere on the collector. The deposition of these particles will be referred to as secondary deposition. The calculations will now be modified to take account of this.

Let the region of no deposition be $(\theta_{1ik}, \theta_{2ik})$, and assume that a fraction γ_{jk} of the particles of size d_j trying to deposit on $(\theta_{1kl}, \theta_{2jk})$ are *not* collected elsewhere on the collector. Equation 70 now becomes

$$A^*_{ij}(\theta) = \chi_{ij} A_{ij}(\theta)\, [1 - (1 - \alpha_{jk})\, \gamma_{jk}] \tag{76}$$

and η^*_{jk-1} becomes

$$\eta^*_{jk-1} = \eta_{jk-1} \frac{[1 - (1 - \alpha_{jk})\, \gamma_{jk}]}{[1 - (1 - \alpha_{jk-1})\gamma_{jk-1}]} \tag{77}$$

It is likely that γ_{jk} is dependent upon the relative sizes of the region of no deposition and the region available for secondary deposition. If the region of no deposition is small compared to the region available for secondary deposition γ_{jk} will also be small (i.e., most of the particles will be deposited). For the reverse situation γ_{jk} will be near unity (i.e., few of the particles will be deposited). Accordingly γ_{jk} will be defined as

$$\gamma_{jk} = (\theta_{2jk} - \theta_{1jk})/(\pi/2 - \theta_{1jk}) \tag{78}$$

The $\bar{\eta}_{ij}$ are arranged in ascending order of magnitude, and P_o and $P_{i_k j}$ defined as before. Thus

$$\eta_j = P_o \eta^*_{jk_1} + \sum_{i=1}^{m} P_{i_k j} \bar{\eta}_{i_k j} \tag{79}$$

A computer program has been written combining the above calculations in order to predict filter performance. Mackie (1984) has shown that the value of $\delta\sigma_i$ is not critical; a value of between 0.0001 and 0.005 is suitable. It is not suggested that these methods of calculation are precise, since many simplifications have been made, some of which are discussed below. However, the work demonstrates that despite the inherent complexity of deep-bed filtration, it is perfectly possible to derive mathematical models that take full account of the relevant factors.

Discussion of the Model

In the development of the model many approximations and simplifications have been made. The validity of these will now be considered.

Use of simplified trajectory analysis

If it is found that simplified trajectory analysis gives inaccurate results for λ_o, then it is suggested that complete trajectory analysis (i.e., including all forces) be used to calculate λ_o. The model described above can then be used to work out the change in λ, i.e., λ/λ_o.

Effect of deposition on the flow field

For small ϵ, perturbation solutions on the flow field can be obtained. For small ϵ Eqs. 40 and 54 give results in good agreement with the perturbation solutions. Details of the comparison can be found in Mackie (1984). Equation 40 predicts that as deposition increases, the amount of fluid flowing between the collector surface and a distance x above the surface increases. This is what one would expect to happen. Equation 54 predicts that v'_θ increases with deposit, a result in accordance with what actually happens in a filter. So Eqs. 40 and 54 give good quantitative results for small ϵ, and good qualitative results for all ϵ.

Other approximations

It should be noted that the methods of accounting for the effect of the region of no deposition, the probability theory, etc., can only be claimed to be qualitatively correct. The actual situation in a filter is so complex that even very sophisticated models by necessity greatly simplify the situation. Therefore their use does not necessarily make the model any better.

Blocking mode

The model assumes that the deposit gradually constricts the pores, whereas there is much evidence that blocking of the pores occurs (Maroudas and Eisenklam, 1965; Payatakes et al., 1981). Also, the constricted-tube models are generally better suited than the Happel model for modeling the later stages of deposition. It therefore should not be surprising if the model proves to require development in order to cope with the final stages of filtration.

The model was tested against a series of experiments (Horner, 1968; Mackie, 1984). At present the values of χ_{ij} and μv^*

have to be calculated empirically. Eventually it should be possible to calculate the value of χ_i mathematically, although v^* may prove more difficult. In the experiment the only conditions that varied from one run to the next were grain size, superficial velocity, and temperature. None of these should affect the values of χ_{ij} and μv^*. If the model developed is a good description of the removal process in filtration, one set of values for χ_{ij} and μv^* should give good agreement between theory and experiment for all the runs executed.

Further applications

Although the model was developed to take account of a suspension of particles of different sizes, the method could also be applied to suspensions consisting of materially different particles. In this case, the value of v^* would be different for each material present. The door is therefore opened to modeling totally general suspensions of the sort encountered in practice.

Experimental Method

Experiments were conducted on a vertical 138 mm dia. filter column. Tapping points arranged in a helical pattern around the filter were used to take samples of the suspensions and to take pressure readings. Ballotini (spherical glass beads) were used as the filter medium, and the artificial suspension was made up from PVC powder (Corvic P 72/757), supplied by ICI England. Four different sizes of ballotini were used in the size ranges defined by B.S. sieves 14–16, 18–22, 22–75, and 30–36. The equivalent mean grain diameters were 1.095, 0.777, 0.653, and 0.458 mm. Experiments were conducted for all four sizes at a superficial velocity of 4.8 m · h^{-1}, and also at 2.4, 3.6, 6.0, and 7.2 m · h^{-1} for size 0.653 mm. The size of the PVC particles varied from less than 0.5 μm up to about 15 μm. Microscopic observation of the suspension showed the particles to be spherical and discrete.

A peristaltic pump was used to pump samples of suspension continuously from each sampling point through 5 mm ID PVC tubing at a constant rate of 100 mL/hour. 20 mL samples for subsequent analysis were collected in test tubes for about 10 min every hour. The samples were analyzed in a Coulter counter TAII, fitted with a population count accessory. The Coulter counter gives data in up to 16 size channels (although in practice only 14 were used as the two smallest channels are subject to electrical noise). This meant that as well as studying the change in total concentration of the suspension with depth and time as it flowed through the filter, the change in concentration of particles of a particular size could also be observed.

Although the Coulter counter gave data in 14 size channels, the number of particles counted in the last two channels (size range 10.08–12.7, and 12.7–16 μm) was usually between 0 and 2, so these channels were ignored in the analysis of the results. In order to reduce statistical errors the remaining 12 channels were split into four groups of three. The size groups were:

Size Group	Size Range, μm
1	0.63–1.26
2	1.26–2.52
3	2.52–5.04
4	5.04–10.98

The experimental conditions are summarized in Tables 1 and 2.

Table 1. Experimental Program

Exp. No.	Grain Size B.S. Sieve	Flow Veloc. m/h	Temp. °C	Porosity	Ag. Conc. mg/L
1	22–25	2.4	18	0.379	216
2	22–25	3.6	18	0.376	197
3	22–25	4.8	19	0.376	170
4	22–25	6.0	19	0.373	160
5	22–25	7.2	19	0.376	100
6	30–36	4.8	23	0.370	100
7	18–22	4.8	23	0.372	197
8	18–22	4.8	23	0.373	212
9	14–16	4.8	22	0.369	264

Experimental Results

The disposition of sampling points is shown in Figure 4. Data from sampling points below point 3 were not used because the concentration values were too low.

All results were corrected to take account of settling in the tubing connecting the sampling points to the peristaltic pump. Investigations showed that settling was negligible for particles in size groups 1 and 2, but very significant for particles in size group 4. In addition, we decided to ignore the results from sampling point 1, which proved to be unrepresentative. In this sampling tube, a sparse matrix of PVC particles was frequently formed. The matrix seemed to emanate from deposited particles dislodged from the filter bed, and although the amount was very small, they appeared to cause the preferential removal of some of the larger particles in the sample suspension, thereby invalidating the results. For this reason we chose to use only the data obtained from sampling points 0, 2, and 3. Further details of this and all other aspects of the experimental work can be found in Mackie (1984).

The results were expressed in the form C_i/C_{oi}, where C_i and C_{oi} are respectively the concentration and inlet concentration of particles in size group 1. Graphs of the variations of C_i/C_{oi} with time were drawn at different filter depths. Figure 5 shows the results obtained for run 3 at a depth of 37 mm, and Figure 6 shows the change in total concentration at that depth. It is immediately clear that the qualitative behavior differs with size group. From the change in overall concentration at $\ell = 37$ mm one would say that the removal efficiency of the first 37 mm of the bed increased for about the first 3 h, and then began to decrease. However, Figure 5 shows that in fact the removal effi-

Table 2. Size Distribution of Inlet Suspension

	% Volume			
	Size Group			
Exp. No.	1	2	3	4
1	13	28	44	15
2	13	29	40	18
3	13	29	37	21
4	13	29	38	20
5	11	30	38	21
6	12	28	34	26
7	14	29	40	18
8	10	23	40	27
9	11	25	41	23

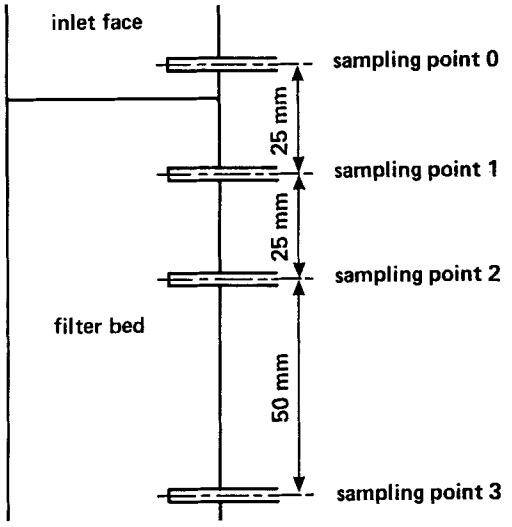

Figure 4. Position of sampling points.

ciency for particles in size groups 1 and 2 increased all the time; the removal efficiency for size group 4 began to decrease after 1 h, and the change in removal efficiency for size group 3 lies somewhere between these two extremes. This behavior was observed throughout the depth of the bed, although the greater the depth, the later the increase in concentration of larger particles. Similar behavior was observed in all the experiments performed. It it therefore apparent that recording the change in total concentration alone does not give a complete picture of what is happening in the filter.

In order to demonstrate the repeatability of the experiments, runs 7 and 8 were performed under almost identical conditions. The results are shown in Figure 7.

Comparison of Theory and Experiment

In order to test the mathematical model, graphs of λ_i vs. σ_i were also drawn. In validating the model, the bed was consid-

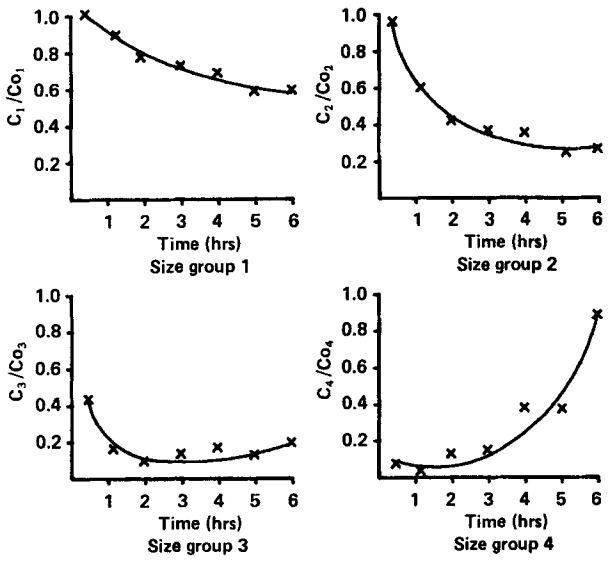

Figure 5. Relative concentrations C_i/Co_i, exp. no. 3.
Size groups 1–4; depth = 37 mm

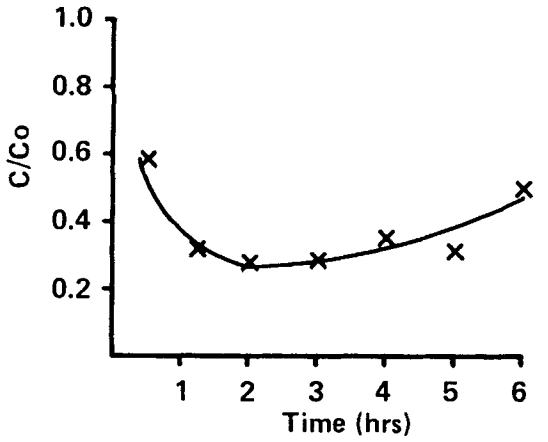

Figure 6. Change in total concentration with time, exp. no. 3.
Depth = 37 mm

ered to be made up of a series of unit bed elements (UBE's), and the change in a layer of fluid elevated as it flowed from one UBE to the next. This allowed us to predict the concentrations of the various particle sizes at the same point in the bed as samples were taken from, and at the same time. The average values of the inlet concentrations observed in the experiments were used in the corresponding simulated filter runs. The theoretical λ_i vs. σ curves were calculated using the predicted values of C_i at the same position as sampling point 2, rather than using the $\lambda_i(\sigma)$ curve obtained for just one UBE. Calculating the theoretical value of λ_i this way means that the average value of λ_i over about 60 UBE's rather than 1 UBE is used. Experimental values of λ_i are also on average value, so it is sensible to use this method to calculate the predicted values of λ_i.

The data input for each computer simulation comprised: grain size, superficial velocity, initial porosity, fluid viscosity, particle and fluid densities, mean size of the particles in size groups 1, 2, 3 and 4, size distribution, and mean inlet concentration.

A value of 0.50 was assumed for the porosity of the deposit. The exact value of f_d is not known, and the choice of value is

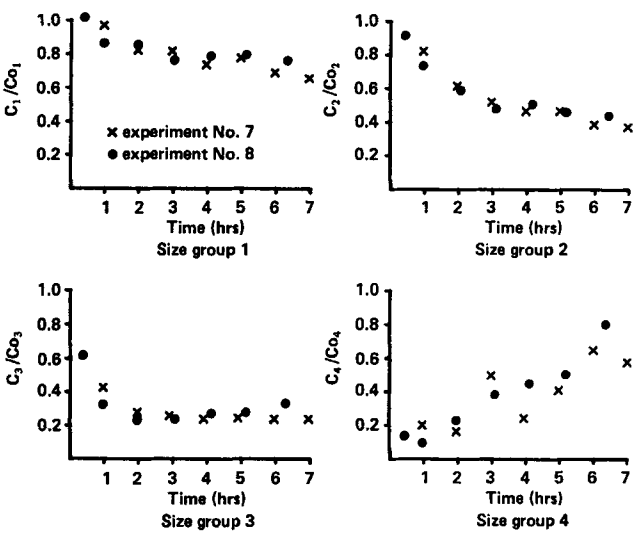

Figure 7. Relative concentration results, exps. 7, 8.

Table 3. Values of χ_{ij}

	j			
i	1	2	3	4
1	1.0	1.0	1.0	1.0
2	1.0	1.0	1.0	1.0
3	0.6	1.0	1.0	1.0
4	0.12	0.6	1.0	1.0

somewhat arbitrary. However, for a similar suspension Horner (1968) quoted a value of 0.569, and Rajagopalan and Tien (1979) have said that to be consistent with a smooth coating mode of deposition, f_d should lie in the range 0.4–0.5. Since our model was a combination of smooth coating and dendritic mode deposition, a value of 0.5 for f_d is not unreasonable. The values of λ_{oi} predicted by simplified trajectory analysis were found to be consistent with the experimental results, so these were used in the model. The values of v^* and χ_{ij} were chosen so that the results predicted by the model gave reasonable agreement with the experimental results for run 3. The values of χ_{ij} are shown in Table 3. The value of v^* was taken to be 0.020 m · s^{-1} at 20°C. The crucial point is that the same values of v^*, χ_{ij}, and f_d were used for all the computer simulations, so that apart from run 3, the model was truly predictive.

Figures 8–12 show typical comparisons of theoretical and experimental results for the $\lambda(\sigma)$ curves for runs 1, 3, 5, and 7 and the C_i/C_{oi} results for run 3. It is clear that the model reflects the qualitative difference in the change of removal efficiency for different particle sizes, and in particular that removal of large particles decreases while removal of small particles is still increasing. The model also predicts the qualitiative effects of changing superficial velocity and grain size on removal efficiency.

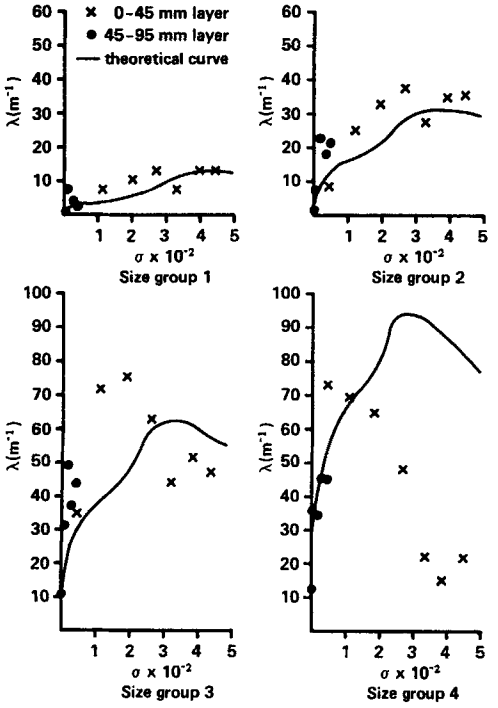

Figure 8. Theoretical and experimental λ vs. σ results, exp. no. 1.

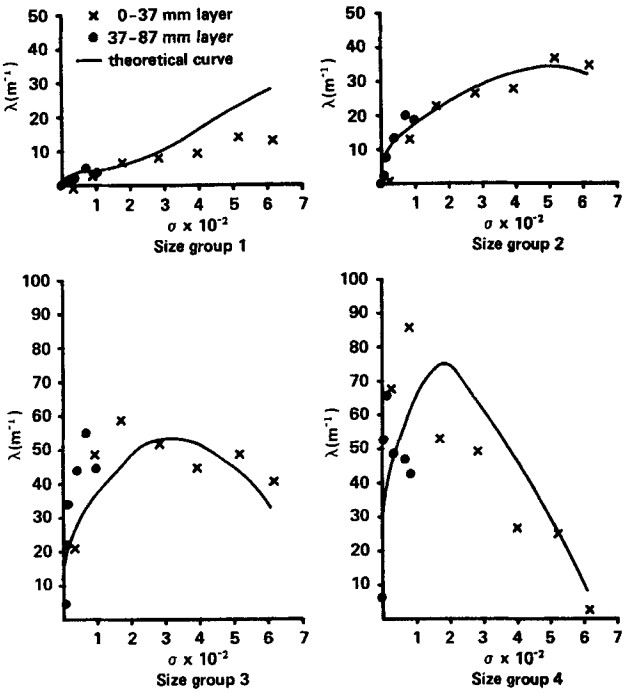

Figure 9. Theoretical and experimental λ vs. σ results, exp. no. 3.

The quantitative results are also reasonable. For size group 1 the predicted values of λ are generally good for $\sigma < 0.025$. However, the model then predicts too large an increase in λ. The agreement for size group 2 is consistently very good. Agreement for group 3 is quite good, although in runs 7, 8, and 9 the model predicts too early a decrease in λ. For size group 4 the model

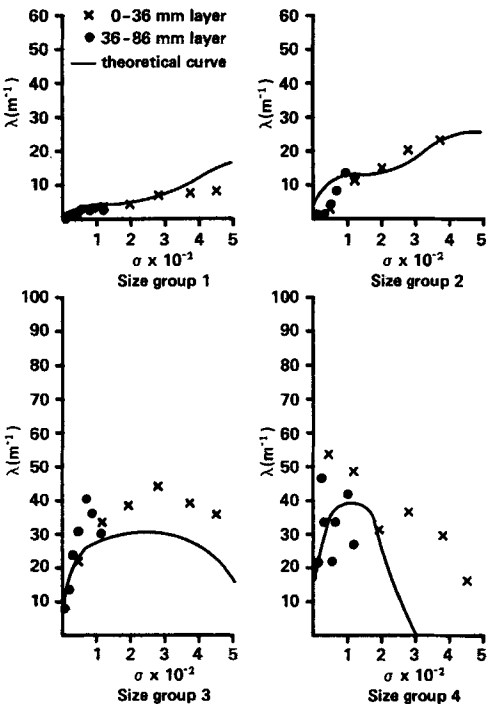

Figure 10. Theoretical and experimental λ vs. σ results, exp. no. 5.

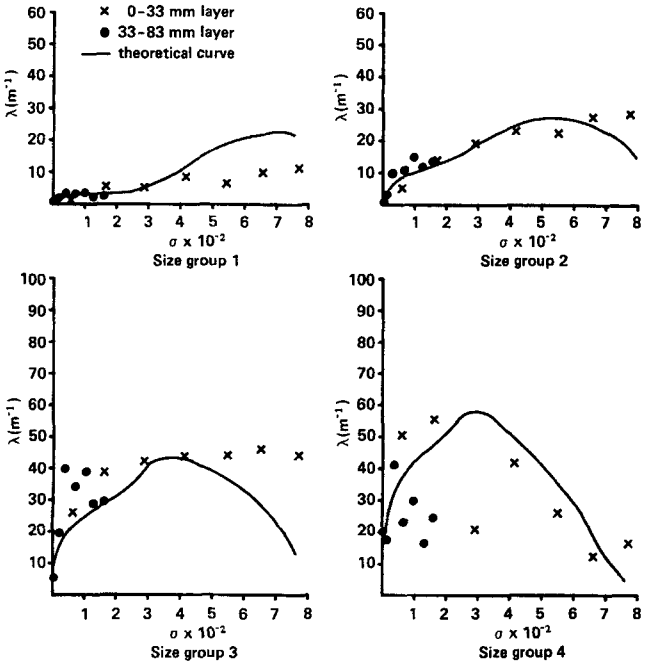

Figure 11. Theoretical and experimental λ vs. σ results, exp. no. 7.

predicts the maximum value of λ fairly well, and for runs 3, 6, 7, and 8 the decrease in λ is accurately predicted. The model predicts too late a decrease in λ_i for runs 1 and 2 and too early a decrease for runs 4 and 5.

Weaknesses of the Model

The model is weakest in the later stages of a filter run. This is not too surprising, since we remarked earlier that the Happel model was not designed to deal with a clogged bed. Nevertheless the fact that the model predicts the qualitative behavior very well and gives good quantitative results much of the time, confirms the principle that increasing tangential fluid velocity near the collector surface is responsible for the decrease in removal efficiency. We conclude therefore that a better method of calculating the increase in tangential fluid velocity is needed, and that it would be advantageous to use a constricted-tube model in the later stages of a filter run.

The model also predicts too rapid an increase in the value of λ for size group 1. This too can be explained by inadequate assessment of the tangential fluid velocity. As deposition takes place, constriction of the pores brings a greater proportion of particles in suspension close to the grain surfaces, thus causing an increase in removal efficiency. At the same time, increases in tangential fluid velocity hinder deposition and counteract the tendency for λ to increase. The results for size group 1 suggest that the model predicts too slow an increase in tangential fluid velocity when σ is quite large (>0.025).

Figure 12 highlights another weakness of the model. For size group 1, the predicted values of C_o/C_{oi} are significantly lower than the experimental values, indicating that the initial increase in λ is overestimated. However, the same problem has been encountered by Chiang and Tien (1983) when using a different method to calculate dendritic deposition, so certainly nothing has been lost. In our model, the answer to this problem may lie with the parameter χ, which characterizes the effect of deposited particles on the local flow field. Although we have assumed χ to be constant during a run and the same for all runs, it is possible that its value depends on the amount of deposition that has taken place. The whole matter requires further mathematical investigation.

Despite these weaknesses, the good agreement between theory and experiment indicates that the principles behind the model are valid. However, there are still factors that the model does not take into account at all. One is the effect of double-layer forces. Rajagopalan and Tien (1977) have shown that as long as double-layer forces are not too large, it is safe to ignore them, but the model as it stands cannot cope with adverse surface force conditions.

A more important point is that the model takes no account of the possibility either of pores being blocked or of deposited particles (or particle clusters) being dislodged although there is considerable evidence to indicate that these events do occur (Payatakes et al., 1981; Maroudas and Eisenklam, 1965; Pendse et al. 1978). We consider that the model should be further developed to take account of the possibility of pore blocking and deposit dislodgement occurring.

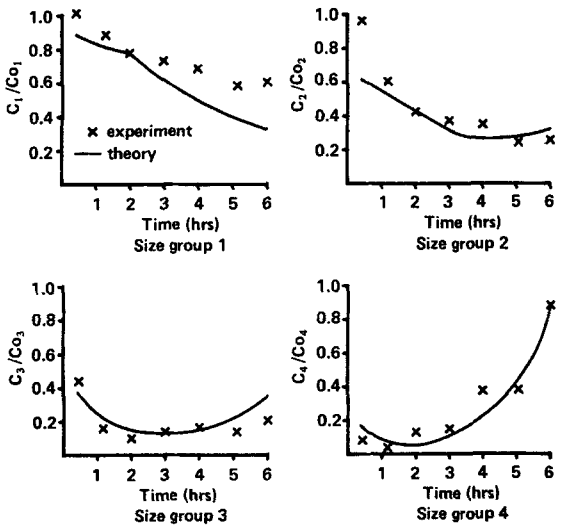

Figure 12. Theoretical and experimental relative concentration, C_i/Co_i, for exp. no. 3.
Size groups 1–4; depth = 37 mm

Acknowledgment

This paper is based on work supported by the Science and Engineering Research Council.

Notation

a = collector radius
a_p = particle radius
A = trajectory parameter
b = radius of outer shell Happel model
C = concentration
d = particle diameter
f_o = porosity of clean filter bed
f_d = porosity of deposit
F_θ = tangential shear force
F_{Lon} = London force
g = acceleration due to gravity
$g(r)$ = function, Eq. 39
$h(r)$ = function, Eq. 50

H = Hamaker constant
I = function, Eq. 74
k_i = constants in stream function, Eq. 5
ℓ = length of bed, or of a UBE
N_G = gravity group
N_I = interception group
p = constant in Happel model, $=a/b$
P_o, P = probabilities
r = radial spherical coordinate
U = superficial velocity for a filter
v_θ = tangential fluid velocity
v^* = critical velocity
V = approach velocity for Happel model
w = constant, $=2 - 3p + 3p^5 - 2p^6$
y_i = "average" height of a sphere
z_o = distance of minimum separation

Greek letters

α = function, Eq. 64
γ_{jk} = function, Eq. 78
δ_θ = area available for flow in Happel model at θ
ϵ = deformation parameter
η = collection efficiency
λ = filter coefficient
μ = viscosity
ϕ = azimuthal coordinate
ρ, ρ_p = fluid and particle densities
σ = specific deposit
ψ = stream function
χ = factors to account for effect of deposited particles on local flow field

Subscripts

i, j = size group i, j
o = initial conditions

Appendix: Relationship Between $\lambda = \eta$ and the Approach Velocity for the Happel Model

In their work with the constricted-tube model, Payatakes et al. (1974b) give the following expression for ℓ:

$$\ell = \left(\frac{4\pi}{3}\right)^{1/3} ap^{-1} \tag{A1}$$

This can be derived by taking ℓ to be the length of the side of the cube that has the same volume as that occupied by one grain in the filter bed. This length ℓ is independent of the type of collector used to represent the filter bed. Therefore the value for ℓ given by Eq. A1 should be used to relate λ and η for the Happel model. Therefore Eq. 2 gives

$$\lambda = -\left(\frac{3}{4\pi}\right)^{1/3} \frac{p}{a} \ln (1 - \eta) \tag{A2}$$

which is not the same as Eq. 11.

For a filter of cross-sectional area A_o the volume of a UBE is ℓA_o. One grain occupies a volume ℓ^3. Therefore the number of grains in the UBE, N, is given by:

$$N\ell^3 = A_o\ell$$
$$N = A_o\ell^{-2}$$

Let V be the approach velocity for the Happel model. Then the flow through each cell is $V\pi a^2p^{-2}$. Therefore the total flow through the UBE is

$$NV\pi a^2p^{-2} = A_o\ell^{-2}\pi a^2p^{-2}V$$

However, the flow through the UBE is also equal A_oU. Therefore

$$A_o\ell^{-2}\pi a^2p^{-2}V = A_oU$$
$$V = \pi^{-1}\ell^2p^2a^{-2}U$$

Using Eq. A1 gives

$$V = \pi^{-1}\left(\frac{4\pi}{3}\right)^{2/3} a^2p^{-2}p^2a^{-2}U$$
$$= \left(\frac{4}{3}\right)^{2/3}\left(\frac{1}{\pi}\right)^{1/3} U \tag{A3}$$

Literature Cited

Chiang, H. W., and C. Tien, "Transient Behavior of Deep-Bed Filters," Symp. Adv. in Solids-Liquid Separ., Univ. College, London (1983).

Goldman, A. J., R. G. Cox, and H. Brenner, "Slow Viscous Motion of a Sphere Parallel to a Plane Wall. I: Motion through a Quiescent Fluid. II: Couette Flow," *Chem. Eng. Sci.*, **22**, 637 (1967).

Happel, J., "Viscous Flow in Multiparticulate Systems: Slow Motion of Fluids Relative to Beds of Spherical Particles," *AIChE J.*, **4**, 197 (1958).

Horner, R. M. W., "Water Clarification and Aquifer Recharge," PhD Thesis, Univ. London (1968).

Ison, C. R., and K. J. Ives, "Removal Mechanisms in Deep-Bed Filtration," *Chem. Eng. Sci.*, **24**, 717 (1969).

Ives, K. J., "Rational Design of Filters," *Proc. Inst. Civ. Eng.*, **16**, 189 (1960).

———, "Rapid Filtration," *Water Res.*, **4**, 201 (1970).

Iwasaki, T., "Some Notes on Sand Filtration," *J. AWWA*, **29**, 1591 (1937).

Mackie, R. I., "Modelling the Effect of Deposition on Removal Efficiency in Deep-Bed Filtration," PhD Thesis, Univ. Dundee (1984).

Maroudas, A., and P. Eisenklam, "Clarification of Suspensions: A Study of Particle Deposition on Granular Media," *Chem. Eng. Sci.*, **20**, 867 (1965).

O'Meilia, C. R., and W. Ali, "The Role of Retained Particles in Deep-Bed Filtration," *Prog. Wat. Technol.*, **10**, 167 (1978).

Payatakes, A. C., "A New Model for Granular Porous Media. Applications to Filtration through Packed Beds," Ph.D. Thesis, Syracuse Univ., New York (1973).

Payatakes, A. C., and C. Tien, "Particle Deposition on Fibrous Media with Dendrite-like Pattern—A Preliminary Model," *J. Aerosol Sci.*, **7**, 85 (1976).

Payatakes, A. C., H. Y. Parks, and J. Petrie, "A Visual Study of Particle Deposition and Reentrainment during Depth Filtration of Hydrosols with a Polyelectrolyte," *Chem. Eng. Sci.*, **36**, 1319 (1981).

Payatakes, A. C., R. Rajagopalan, and C. Tien, "Application of Porous Media Models to the Study of Deep-Bed Filtration," *Can. J. Chem. Eng.*, **52**, 722 (1974a).

Payatakes, A. C., C. Tien, and R. M. Turian, "Trajectory Calculation of Particle Deposition in Deep Bed Filtration. I: Model Formulation. II: Case Study of the Effect of Dimensionless Groups and Comparison with Experimental Data," *AIChE J.*, **20**, 889 (1974b).

Pendse, H., C. Tien, R. M. Turian, and R. Rajagopalan, "Dispersion Measurements in Clogged Filter Beds—A Diagnostic Study of the Morphology of Particle Deposition," *AIChE J.*, **24**, 473 (1978).

Rajagopalan, R., and J. S. Kim, "Adsorption of Brownian Particles in the Presence of Potential Barriers: Effect of Different Modes of Double-Layer Interaction," *J. Colloid Interf. Sci.*, **83**, 428 (1981).

Rajagopalan, R., and C. Tien, "Trajectory Analysis of Deep-Bed Filtration with the Sphere-in-Cell Porous Media Model," *AIChE J.*, **22**, 523 (1976).

———, "Analysis of Collection Mechanisms in Water Filtration," *Can J. Chem.*, **55**, 246 (1977).

———, "The Theory of Deep-Bed Filtration," *Progressd in Filtration and Separation*, R. J. Wakeman, ed., Elsevier, Amsterdam (1979).
Spielman, L. A., and J. A. FitzPatrick, "Theory for Particle Collection under London and Gravity Forces," *J. Colloid. Interf. Sci.*, **42**, 607 (1973).
Stein, P. C., "A Study of the Theory of Rapid Filtration of Water through Sand," D.Sc. Diss., Mass. Inst. Tech., Cambridge (1940).
Tien, C., and A. C. Payatakes, "Advances in Deep-Bed Filtration," *AIChE J.*, **25**, 737 (1979).
Tien, C., R. M. Turian, and H. Pendse, "Simulation of the Dynamic Behavior of Deep-Bed Filters," *AIChE J.*, **25**, 385 (1979).
Vankatasan, M., and R. Rajagopalan, "A Hyperboloidal Constricted-Tube Model for Porous Media," *AIChE J.*, **26**, 694 (1980).
Visser, J., "The Adhesion of Colloidal Polystyrene Particles in Cellophane as a Function of pH and Ionic Strength," *J. Colloid Interf. Sci.*, **55**, 664 (1976).
Wang, C. S., M. Beizaie, and C. Tien, "Deposition of Solid Particles on a Collector: Formulation of a New Theory," *AIChE J.*, **23**, 879 (1977).
Wnek, W. J., D. Gidaspow, and T. Wasan, "The Role of Colloidal Chemistry in the Modeling of Deep-Bed Filtration," *Chem. Eng. Sci.*, **30**, 1035 (1975).
Yao, K. M. "Influence of Particle Size on the Transport Aspect of Water Filtration," Ph.D. Thesis, Univ. of North Carolina, Chapel Hill (1968);

Manuscript received June 5, 1986, and revision received Mar. 9, 1987.